Supplementary Materials

A 3D ordered hierarchical crystalline porous organic salt for large-sized enzyme immobilization

Jinman Wang[1], Guolong Xing[1,2,3,*], Yu Zhao[1,3], Jinming Zhou[3], Bo Song[2,4], Li-Hua Chen[5], Weidong Zhu[1,3], Bao-Lian Su[5,6,*], Teng Ben[1,2,3,*]

[1]Zhejiang Engineering Laboratory for Green Syntheses and Applications of Fluorine-Containing Specialty Chemicals, Institute of Advanced Fluorine-Containing Materials, Zhejiang Normal University, Jinhua 321004, Zhejiang, China.
[2]Science and Technology Center for Quantum Biology, National Institute of Extremely-Weak Magnetic Field Infrastructure, Hangzhou 310000, Zhejiang, China.
[3]Key Laboratory of the Ministry of Education for Advanced Catalysis Materials, Institute of Physical Chemistry, Zhejiang Normal University, Jinhua 321004, Zhejiang, China.
[4]School of Optical-Electrical Computer Engineering, University of Shanghai for Science and Technology, Shanghai 200093, China.
[5]Laboratory of Living Materials at the State Key Laboratory of Advanced Technology for Materials Synthesis and Processing, Wuhan University of Technology, Wuhan 430070, Hubei, China.
[6]Laboratory of Inorganic Materials Chemistry, University of Namur, Namur B-5000, Belgium.

[*]**Correspondence to:** Dr. Guolong Xing, Prof. Teng Ben, Zhejiang Engineering Laboratory for Green Syntheses and Applications of Fluorine-Containing Specialty Chemicals, Institute of Advanced Fluorine-Containing Materials, Zhejiang Normal University, Yingbin Road 688, Jinhua 321004, Zhejiang, China. E-mail: xinggl@zjnu.edu.cn; tengben@zjnu.edu.cn; Prof. Bao-Lian Su, Laboratory of Inorganic Materials Chemistry, University of Namur, Rue de Bruxelles 61, Namur B-5000, Belgium. E-mail: bao-lian.su@unamur.be

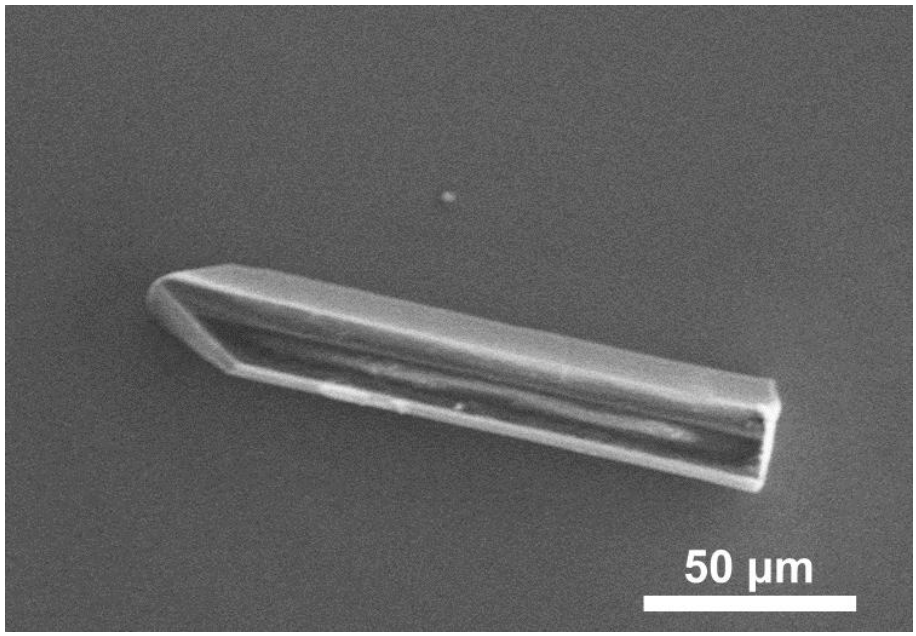

Supplementary Figure 1. SEM image of CPOS-1-Cryst.

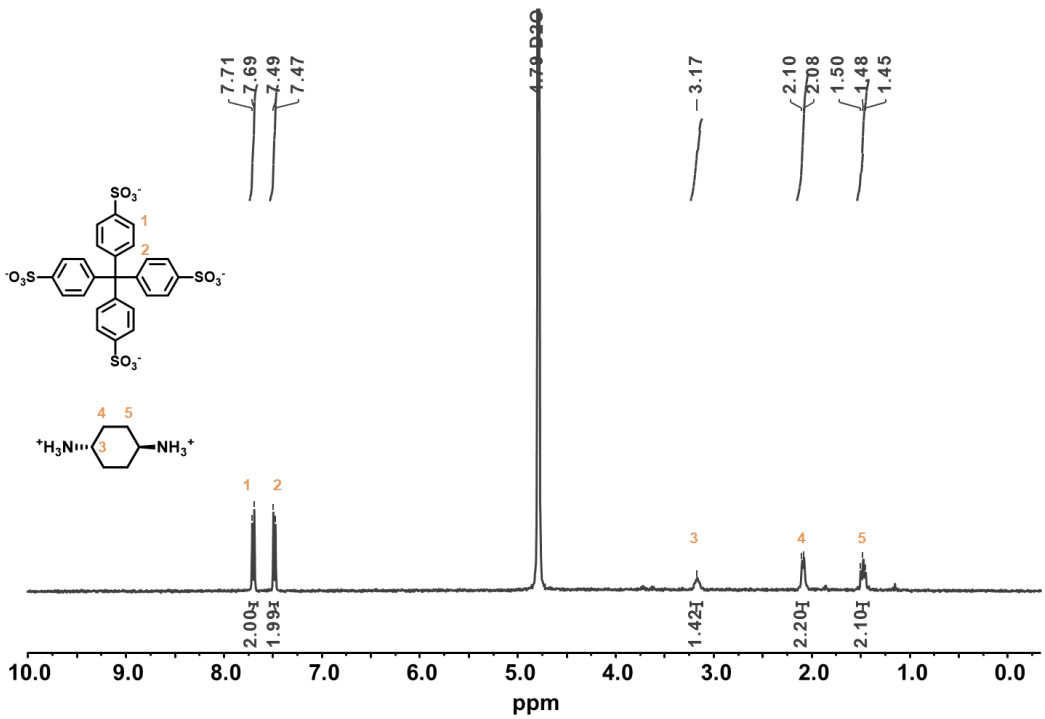

Supplementary Figure 2. ^{1}H NMR spectrum of CPOS-1-Cryst.

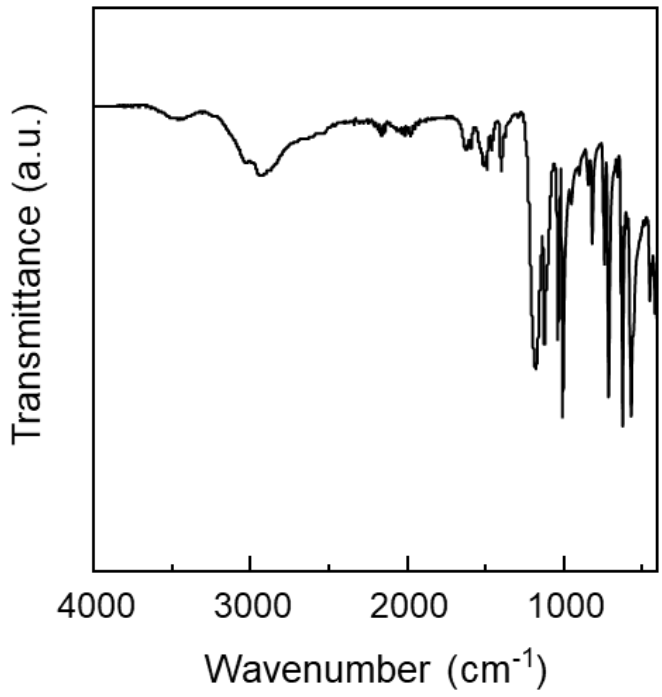

Supplementary Figure 3. FT-IR spectrum of CPOS-1-Cryst.

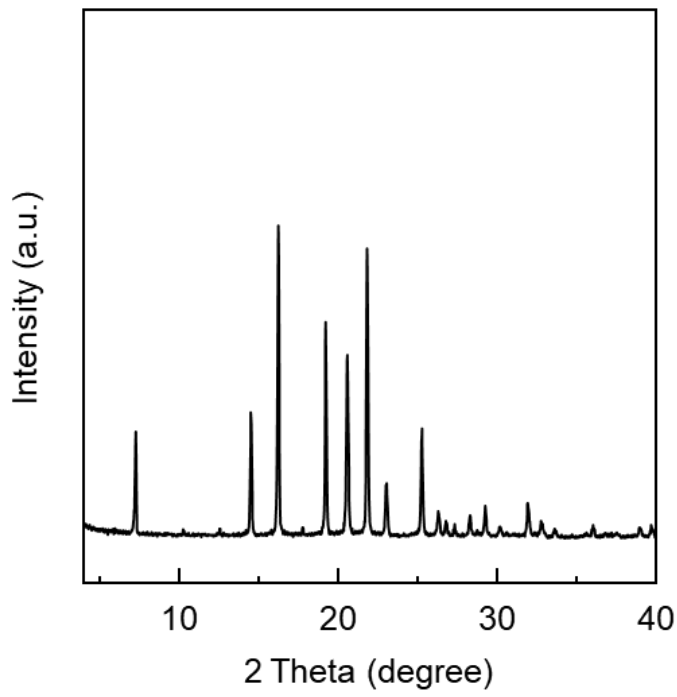

Supplementary Figure 4. PXRD pattern of CPOS-1-Cryst.

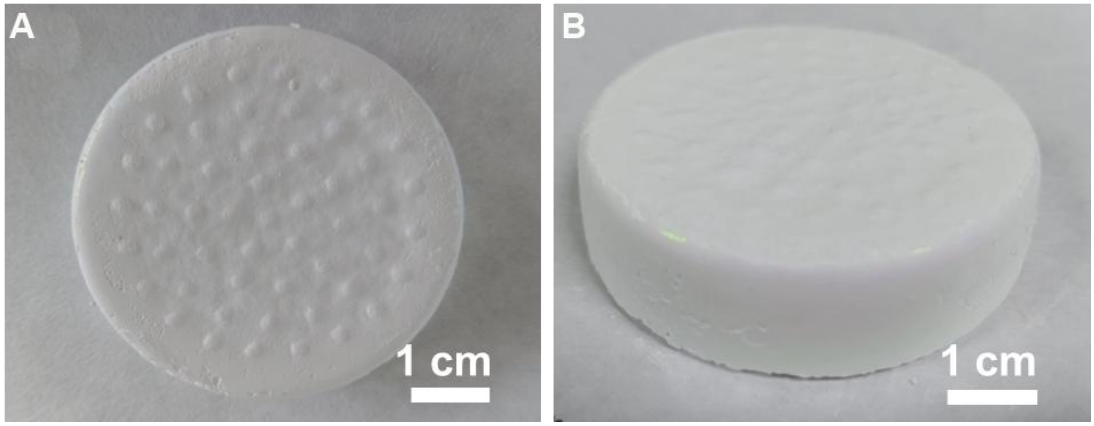

Supplementary Figure 5. Photographs of 3D ordered PS colloidal crystal template.

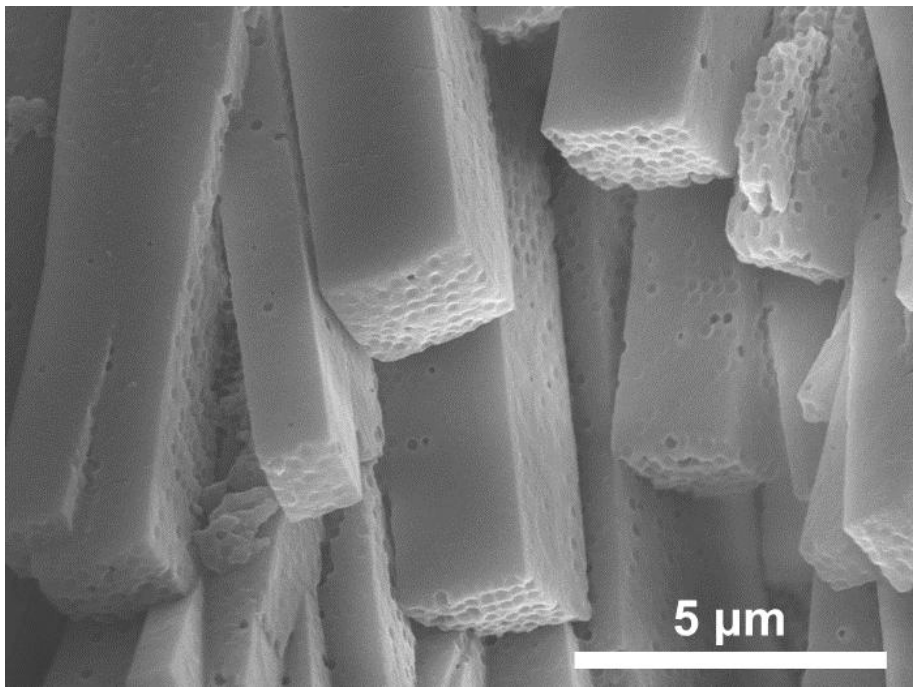

Supplementary Figure 6. SEM image of CPOS-1 with discrete macropore on the surface.

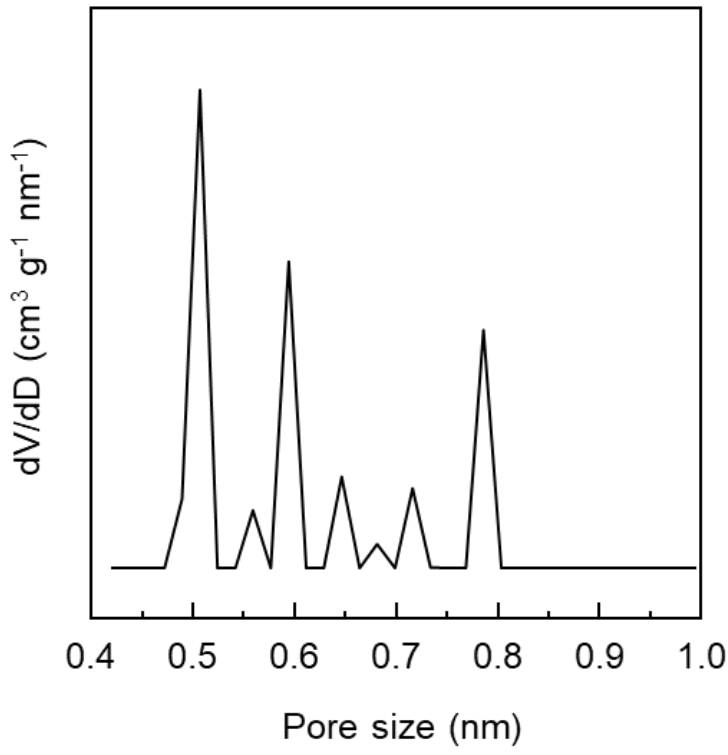

Supplementary Figure 7. Pore size distribution of HCPOS-1.

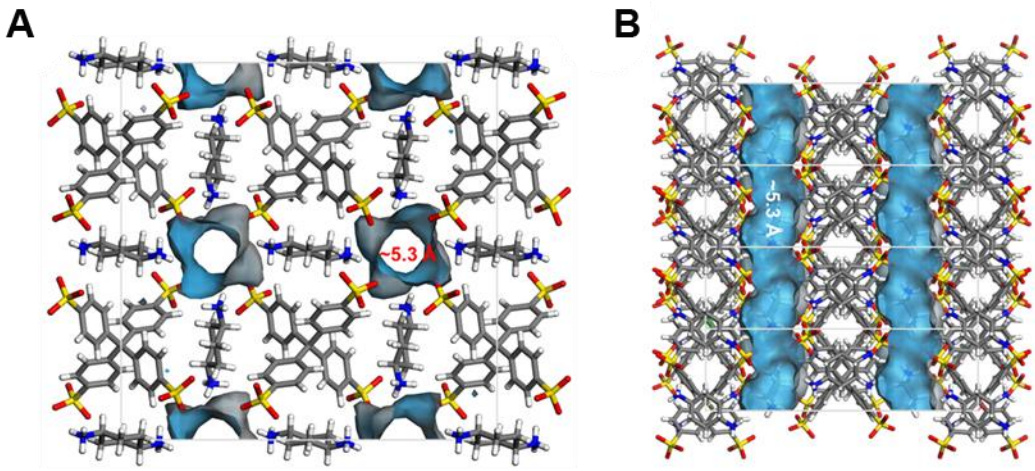

Supplementary Figure 8. (A) The top view and (B) the side view of CPOS-1 structure.

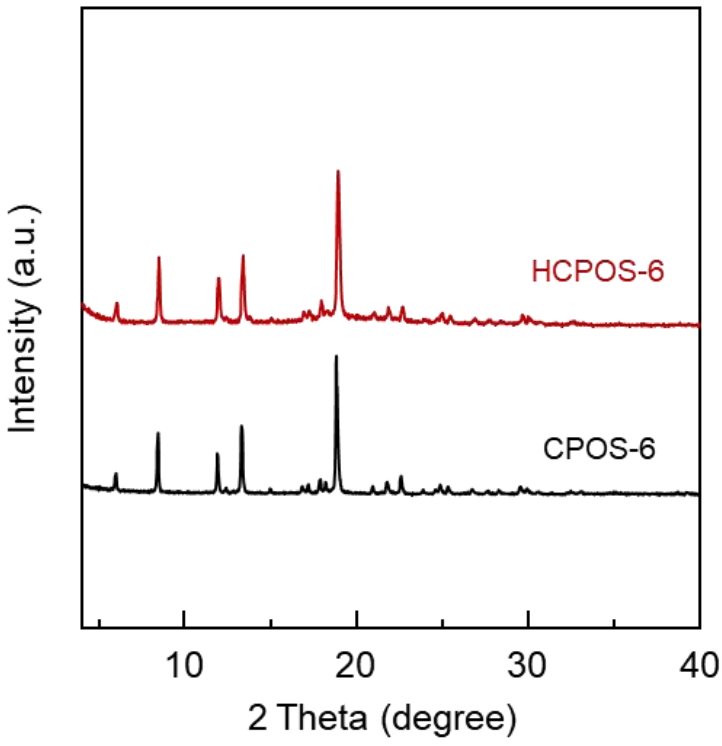

Supplementary Figure 9. PXRD patterns of CPOS-6 and HCPOS-6.

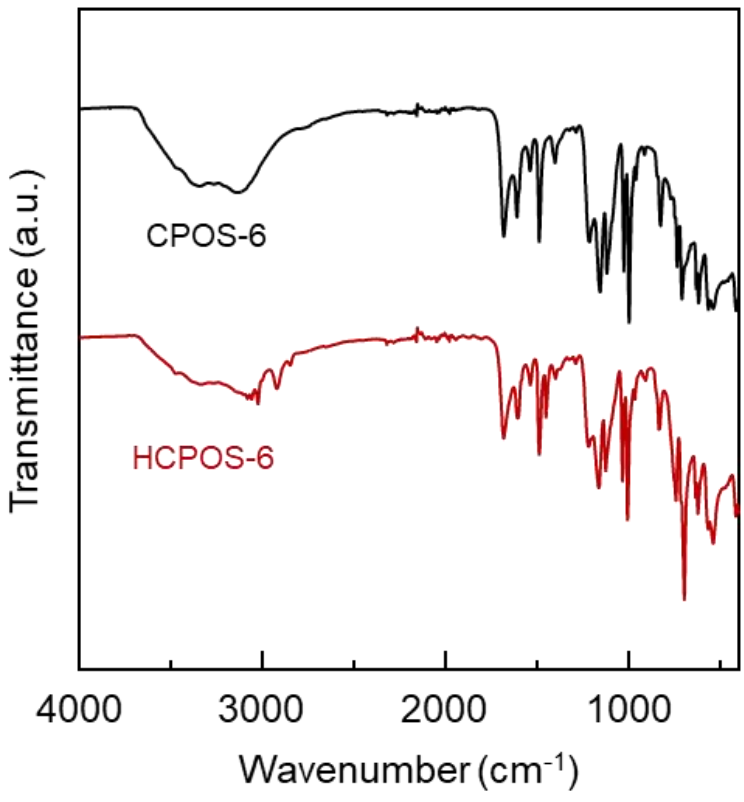

Supplementary Figure 10. IR spectra of CPOS-6 and HCPOS-6.

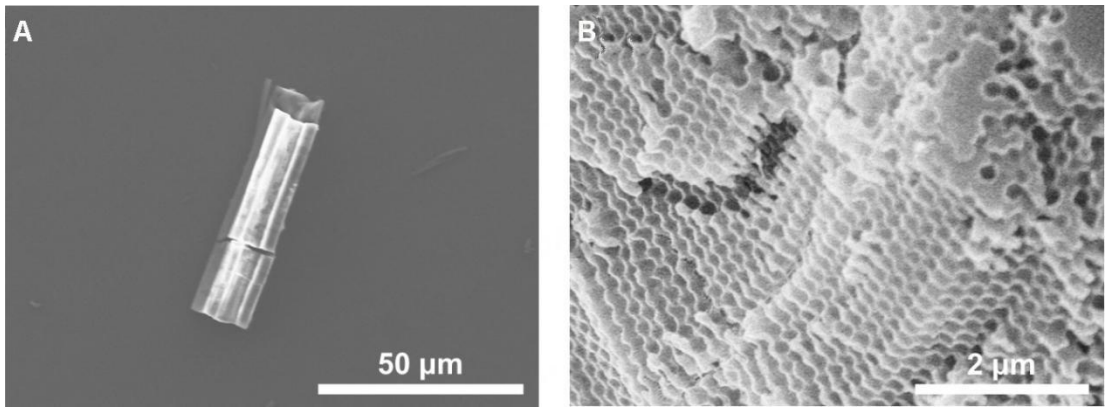

Supplementary Figure 11. SEM images of (A) CPOS-6 and (B) HCPOS-6.

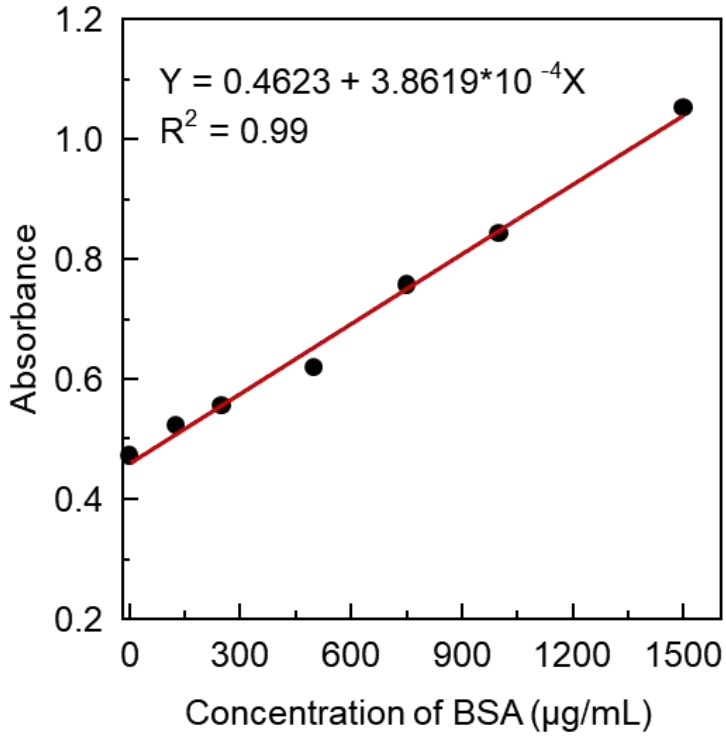

Supplementary Figure 12. The calibration curve of BSA concentration based on Bradford assay.

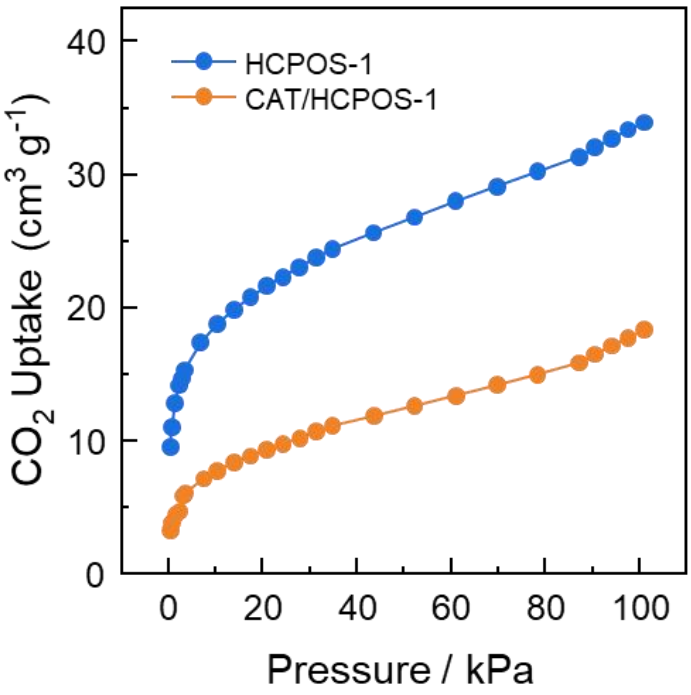

Supplementary Figure 13. CO_2 sorption isotherms of CAT/HCPOS-1 and HCPOS-1 at 273 K.

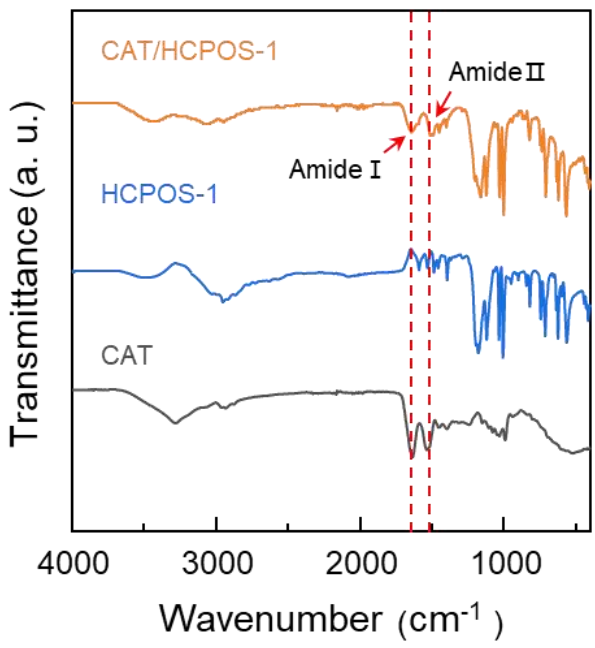

Supplementary Figure 14. FT-IR spectra of CAT/HCPOS-1, HCPOS-1 and CAT.

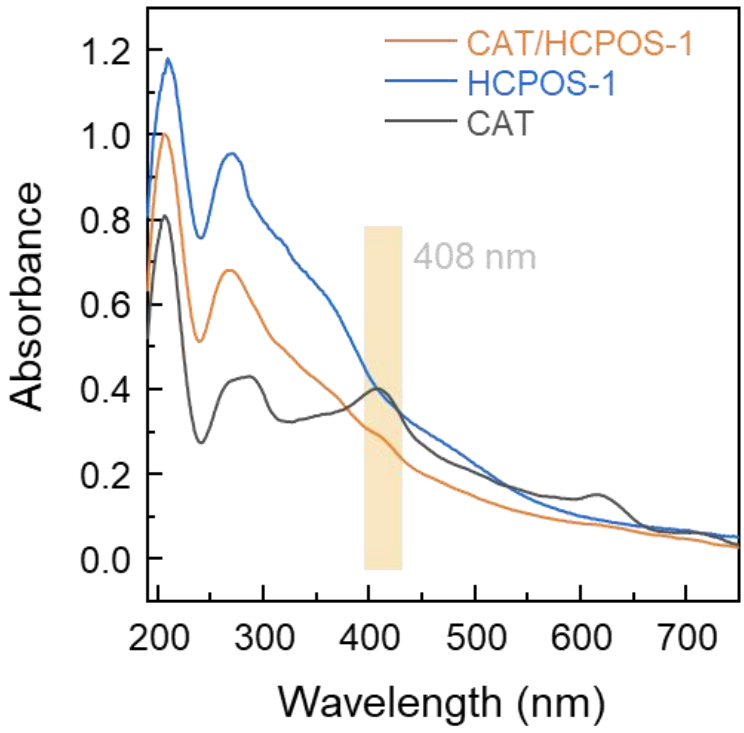

Supplementary Figure 15. Solid-state UV-Visible spectra of CAT/HCPOS-1, HCPOS-1 and CAT.

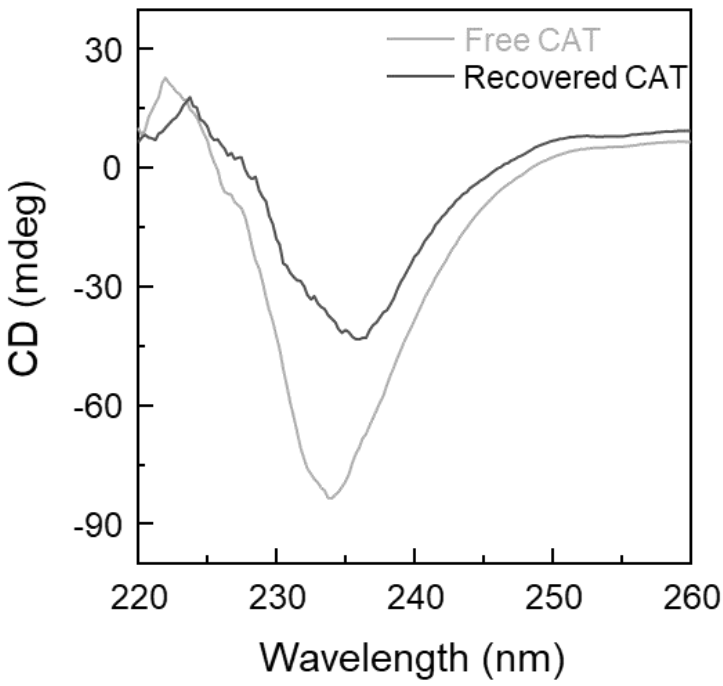

Supplementary Figure 16. CD spectra of free CAT and recovered CAT from CAT@HCPOS-1. Directly putting CAT@HCPOS-1 into PBS buffer (pH = 7.4, 3 mM) to get recovered CAT.

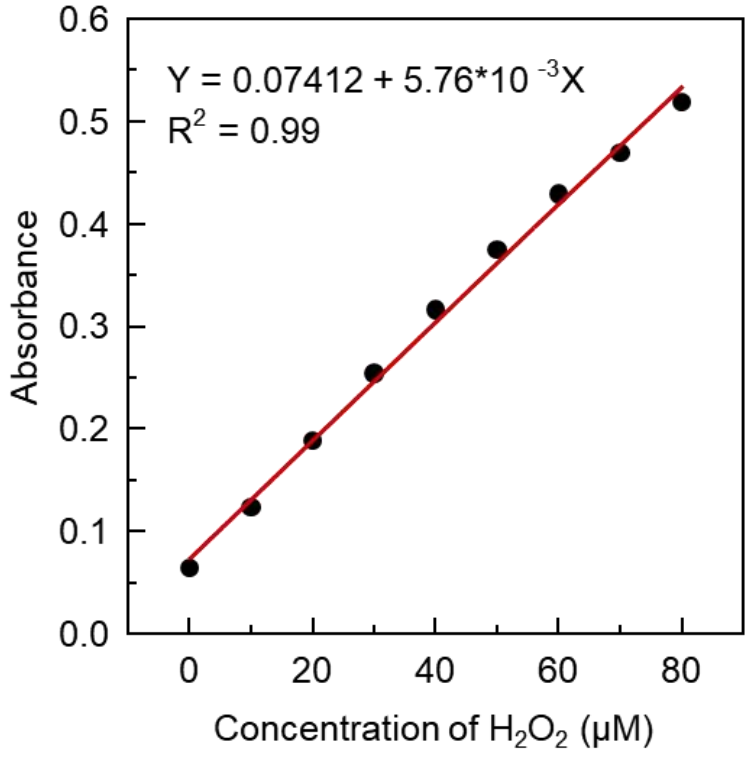

Supplementary Figure 17. The calibration curve of H_2O_2 concentration based on FOX (Ferrous Oxidation in Xylenol orange) assay. Briefly, H_2O_2 standard solutions (50 μL) at various concentrations were mixed with the FOX reagent (composed of 250 μM ammonium ferrous sulfate, 100 μM xylenol orange, and 100 mM sorbitol in 25 mM H_2SO_4; 950 μL) and incubated for 30 min at room temperature before reading absorbance at 560 nm.

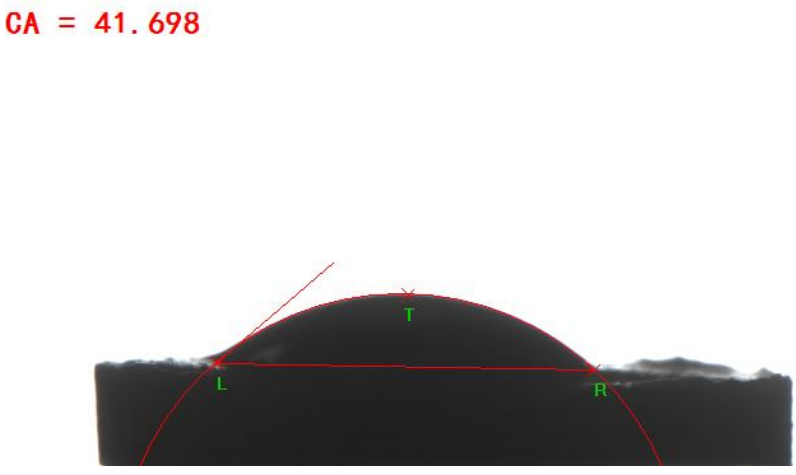

Supplementary Figure 18. Water contact angle of HCPOS-1.

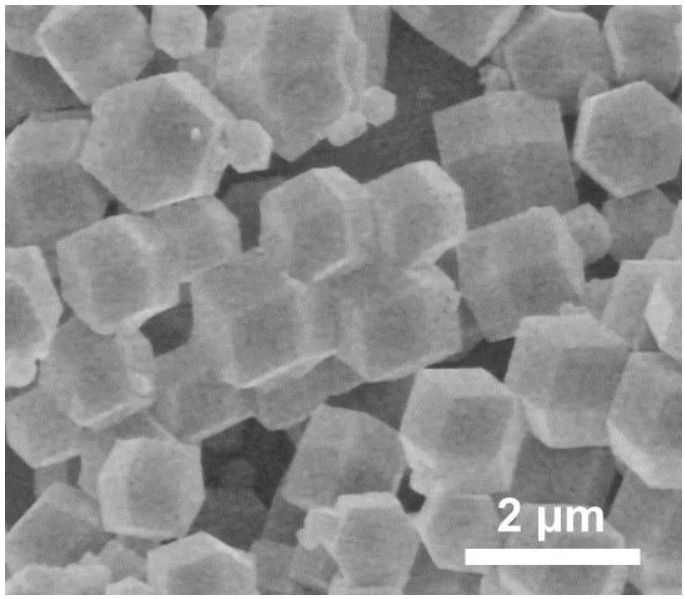

Supplementary Figure 19. SEM image of ZIF-8.

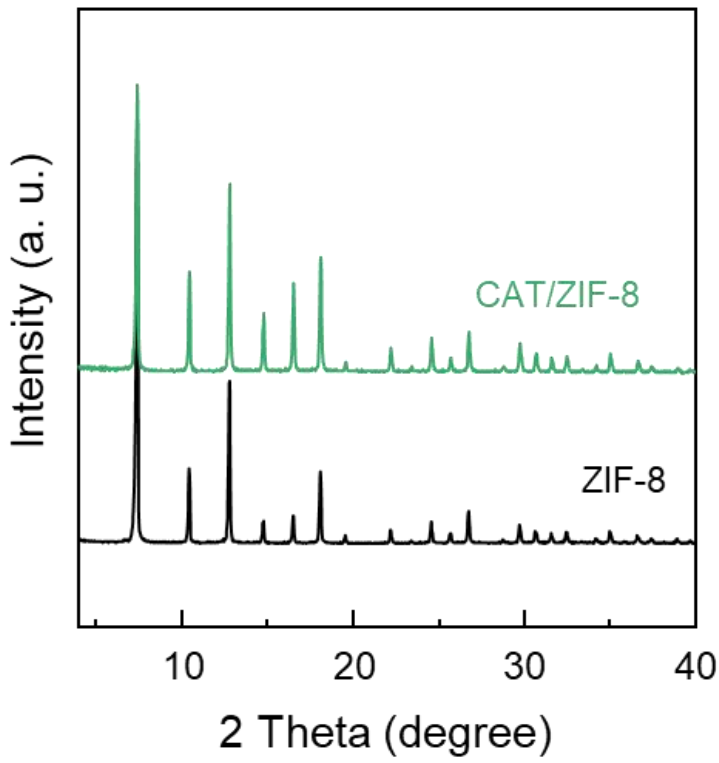

Supplementary Figure 20. PXRD patterns of CAT/ZIF-8 and ZIF-8.

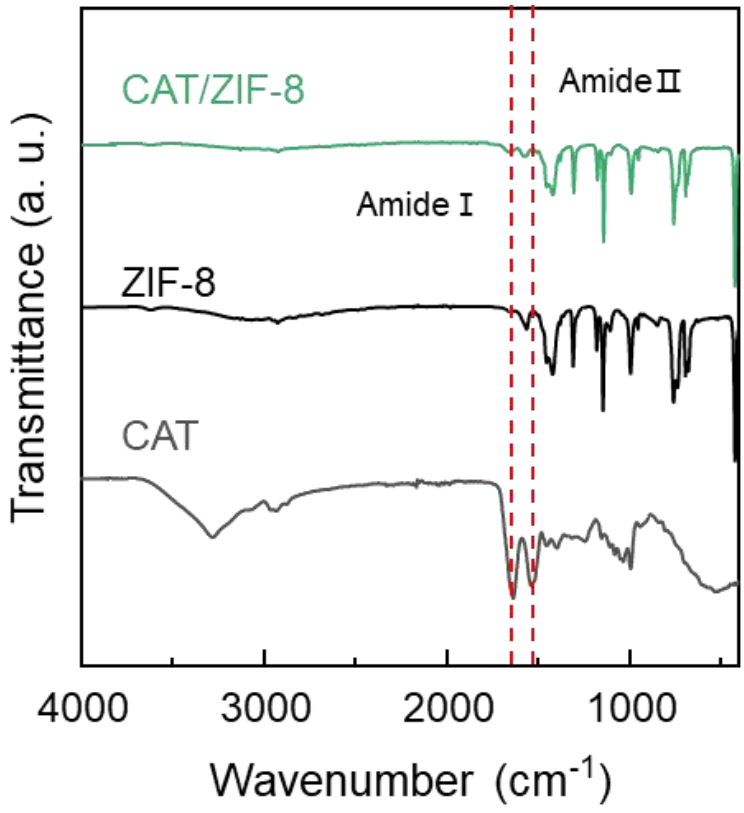

Supplementary Figure 21. FT-IR spectra of CAT/ZIF-8, ZIF-8 and CAT.

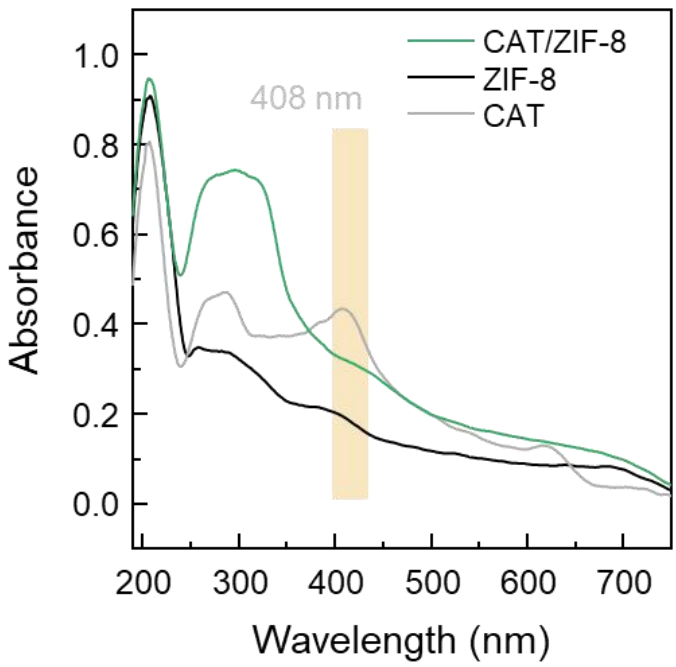

Supplementary Figure 22. Solid-state UV-visible spectra of CAT/ZIF-8, ZIF-8 and CAT.

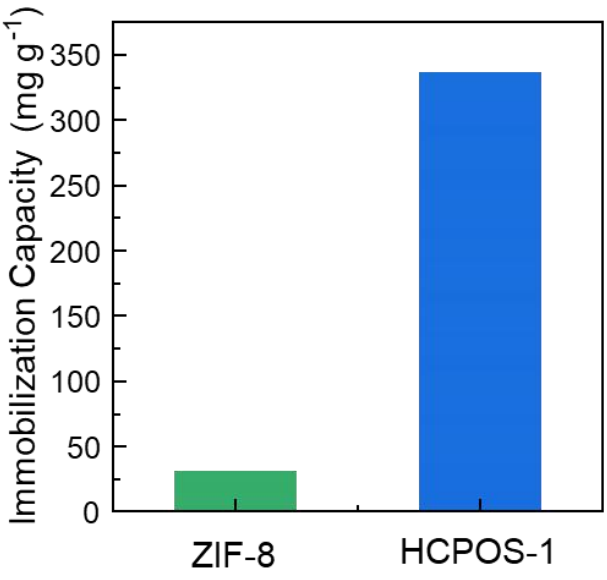

Supplementary Figure 23. The enzyme immobilization capacities of ZIF-8 and HCPOS-1.

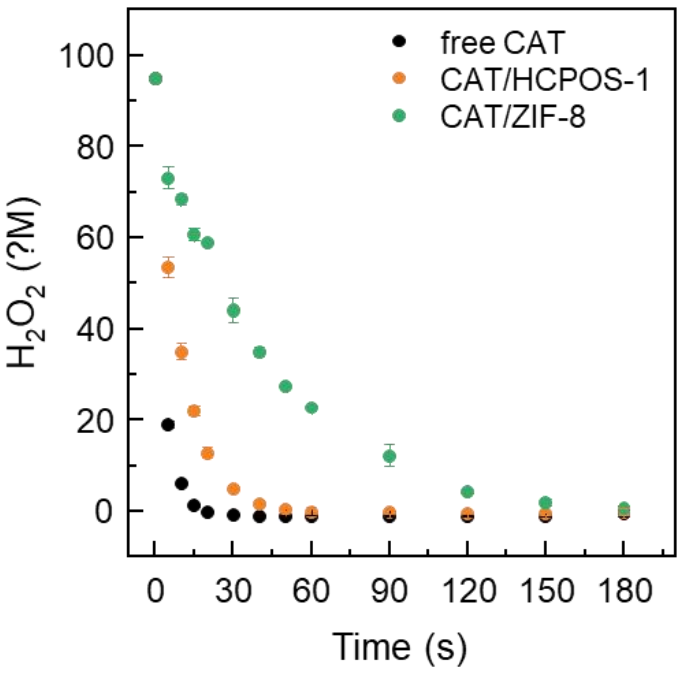

Supplementary Figure 24. Catalytic performance of CAT/HCPOS-1 and CAT/ZIF-8. The assay was performed in Tris-HCl buffer (pH 8, 50 mM) with H_2O_2 (0.095 mM) and encapsulated CAT that determined by Bradford assay (50 μg).

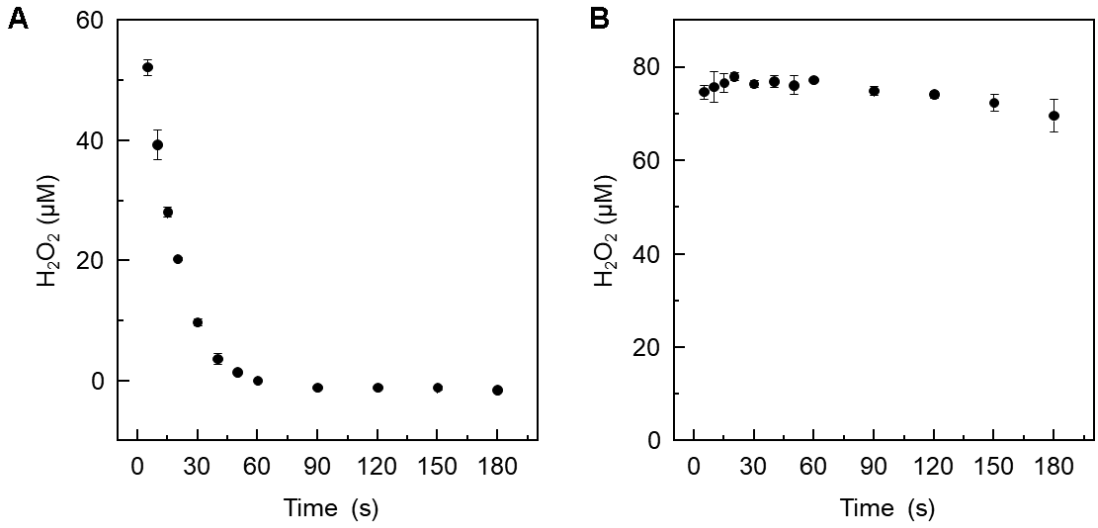

Supplementary Figure 25. The catalytic stability of CAT/HCPOS-1. (A) first cycle and (B) second cycle.

Supplementary Table 1. Comparison of immobilization capacity of HCPOS-1 with reported porous organic frameworks

Enzyme	Materials	Immobilization method	Immobilization capacity (mg g^{-1})	Ref.
CAT	mNMZIF-8	Covalent binding and cross-linking	1000.0	[1]
GOx	MOF-545(Fe)	Pore encapsulation	296.0	[2]
CAT	MAF-7	Physical adsorption	5.0	[3]
CAT	MAF-7	*In situ* encapsulation	9.1	[3]
CAT	BioHOF-1	*In situ* encapsulation	60.0	[4]
GDH	ZIF-67	Physical adsorption	110.4	[5]
GDH	ZIF-8	Physical adsorption	88.3	[5]
Trypsin	UiO-66(Zr)	Physical adsorption	80.2	[6]
	CYCU-4(Al)	Physical adsorption	163.4	[6]
Cyt *c*	ZIF-8	Physical adsorption	71.0	[7]
CAT	Zr-fcu-azo/sti-30%	Pore encapsulation	210.0	[8]
GOx	PCN-888-en	Pore encapsulation	1000.0	[9]
HRP	PCN-888-en	Pore encapsulation	2000.0	[9]
Z-DAAO	BioHOF-1	*In situ* encapsulation	500.0	[10]
CAT	HCPOS-1	Physical adsorption	336.9	This work
CAT	CPOS-1	Physical adsorption	163.3	This work
CAT	ZIF-8	Physical adsorption	31.7	This work

REFERENCES

1. Feng Y, Hu H, Wang Z, et al. Three-dimensional ordered magnetic macroporous metal-organic frameworks for enzyme immobilization. *J Colloid Interface Sci* 2021; 590: 436-45. https://doi.org/10.1016/j.jcis.2021.01.078
2. Zhong X, Xia H, Huang W, Li Z, Jiang Y. Biomimetic metal-organic frameworks mediated hybrid multi-enzyme mimic for tandem catalysis. *Chem Eng J* 2020; 381: 122758. https://doi.org/10.1016/j.cej.2019.122758
3. Liang W, Xu H, Carraro F, et al. Enhanced activity of enzymes encapsulated in hydrophilic metal-organic frameworks. *J Am Chem Soc* 2019; 141: 2348-55. https://doi.org/10.1021/jacs.8b10302
4. Liang W, Carraro F, Solomon MB, et al. Enzyme encapsulation in a porous hydrogen-bonded organic framework. *J Am Chem Soc* 2019; 141: 14298-305. https://doi.org/10.1021/jacs.9b06589
5. Ma W, Jiang Q, Yu P, Yang L, Mao L. Zeolitic imidazolate framework-based electrochemical biosensor for in vivo electrochemical measurements, *Anal Chem* 2013; 85: 7550-7. https://doi.org/10.1021/ac401576u
6. Liu W, Wu C, Chen C, Singco B, Lin CH, Huang HY. Fast multipoint immobilized MOF bioreactor. *Chem Eur J* 2014; 20: 8923-8. https://doi.org/10.1002/chem.201400270
7. Zhang C, Wang X, Hou M, Li X, Wu X, Ge J. Immobilization on metal−organic framework engenders high sensitivity for enzymatic electrochemical detection. *ACS Appl Mater Interfaces* 2017; 9: 13831-6. https://doi.org/10.1021/acsami.7b02803
8. Yang Y, Arque X, Patino T, et al. Enzyme-powered porous micromotors built from a hierarchical micro- and mesoporous UiO-type metal−organic framework. *J Am Chem Soc* 2020; 142: 20962-7. https://doi.org/10.1021/jacs.0c11061
9. Lian X, Chen Y, Liu T, Zhou H. Coupling two enzymes into a tandem nanoreactor utilizing a hierarchically structured MOF. *Chem Sci* 2016; 7: 6969-73. https://doi.org/10.1039/C6SC01438K
10. Wied P, Carraro F, Bolivar JM, Doonan CJ, Falcaro P, Nidetzky B. Combining a genetically engineered oxidase with hydrogen-bonded organic frameworks (HOFs) for highly efficient biocomposites. *Angew Chem Int Ed* 2022; 61: e202117345. https://doi.org/10.1002/anie.202117345